Photochemistry and Photobiology, 2017, 93: 1312–1319

Marine Bioluminescence: Measurement by a Classical Light Sensor and Related Foraging Behavior of a Deep Diving Predator†

Jade Vacquié-Garcia*‡[1], Jérôme Mallefet[2], Frédéric Bailleul[3], Baptiste Picard[1] and Christophe Guinet[1]

[1]Centre d'Etudes Biologiques de Chizé, CNRS, Villiers en Bois, France
[2]Université catholique du Louvain, UCL, Louvain-la-Neuve, Belgique
[3]South Australian Research and Development Institute (Aquatic Sciences), Adelaide, SA, Australia

Received 11 September 2016, accepted 14 March 2017, DOI: 10.1111/php.12776

ABSTRACT

Bioluminescence is produced by a broad range of organisms for defense, predation or communication purposes. Southern elephant seal (SES) vision is adapted to low-intensity light with a peak sensitivity, matching the wavelength emitted by myctophid species, one of the main preys of female SES. A total of 11 satellite-tracked female SESs were equipped with a time-depth-light 3D accelerometer (TDR10-X) to assess whether bioluminescence could be used by SESs to locate their prey. Firstly, we demonstrated experimentally that the TDR10-X light sensor was sensitive enough to detect natural bioluminescence; however, we highlighted a low-distance detection of the sensor. Then, we linked the number of prey capture attempts (PCAs), assessed from accelerometer data, with the number of detected bioluminescence events. PCA was positively related to bioluminescence, which provides strong support that bioluminescence is involved in predator–prey interactions for these species. However, the limitations of the sensor did not allow us to discern whether bioluminescence (i) provided remote indication of the biological richness of the area to SES, (ii) was emitted as a mechanic reaction or (iii) was emitted as a defense mechanism in response to SES behavior.

INTRODUCTION

Bioluminescence is defined by the production and emission of light by a living organism (1). In the vast majority of bioluminescent marine organisms, the spectral range of bioluminescence is limited to blue/green wavelengths, centered around 470 to 500 nm (2). Due to sophisticated control mechanisms to produce precise patterns of light emission (flashes and glows), it is commonly assumed that bioluminescence increases the emitter's fitness in at least three critical ways: (i) it is essential as a defense against predators (defensive function); (ii) it is used in food acquisition by means of, for example, a lure or built-in headlights (offensive function); and (iii) it allows to attract a mate by means of species-specific spatial or temporal patterns of light emission (matching function) (1,3). The defensive function, the most common use of bioluminescence, takes many forms such as startling, sacrificial lure or counter illumination (i.e. the silhouette of an animal seen by a predator coming from under is concealed by the ventral bioluminescence of same color, intensity and angular distribution of the residual ambient light). However, bioluminescence emitted by an organism can also be "diverted" by others organisms not targeted by the emissions; in that case, the beneficiary of the emissions might not be the emitter (e.g. a visual predator taking advantage of the bioluminescence emitted by the prey to catch it).

The presumed functions of the light emission are generally deduced from morphological and physiological characteristics observed *ex situ* rather than from *in situ* studies or observations (4). As an example, the defensive function based on counter illumination has been mainly investigated during *ex situ* experiments, where the ability of organisms to adjust their light ventral emissions to match light characteristics of artificially manipulated light fields has been highlighted (5–8). Behavioral experiments on the role of the bioluminescence exist, such as those demonstrating that dinoflagellate bioluminescence reduces grazing by copepods by attracting top predators (5,9,10). However, they remain extremely rare probably because the direct observation of bioluminescence *in situ* still represents a challenge for scientists. The use of remote-operated vehicles, submersibles or video profilers constitutes a valuable opportunity to explore the deep ocean. These instruments reveal the existence of new luminescent organisms. They also reveal the vertical distribution of bioluminescent organisms within the water column as well as the spatial variation in bioluminescence activity (11–13). However, in the vast majority of cases, due to the size and noise generated by the equipment, they remain of limited value to properly investigate natural behaviors or interactions between the organisms. In the last decades, studies deploying irradiance time-depth recorders on marine predators were able to sample the luminescent field to which these animals were exposed (14,15). The use of such devices represents then an interesting alternative to observe bioluminescence *in situ* and to better understand the interspecific interactions based on bioluminescence.

Southern elephant seal (SES hereafter), *Mirounga leonina*, spends 10 months per year feeding at sea and come back ashore only to breed in October, or to molt in January. When foraging at sea, SES travels large distances and dives almost continuously, performing on average 60 dives per day. They dive in the

*Corresponding author email: jadevacquiegarcia@gmail.com (Jade Vacquié-Garcia)
†This article is a part of the Special Issue devoted to various aspects of basic and applied research on bioluminescence.
‡Current address: Jade Vacquié-Garcia, Norwegian Polar Institute, Fram Centre, Tromsø, Norway

mesopelagic zone to about 600 m depth where they encounter bioluminescence (15). Nitrogen stable isotope analyses revealed that bioluminescent myctophids were one of the most dominant components of the diet of females SES from Kerguelen Islands (16). Bioluminescent myctophids are extremely abundant in the mesopelagic zone, their peak eye sensitivity ranges from 450 to 480 nm (2), and their maximal wavelength emission ranges from 450 to 480 nm depending on the species (17–19), suggesting a wavelength range overlap in the spectral eye sensitivity and bioluminescence. The bioluminescence functions of these fish are not completely understood but dimorphism (sex- and species-specific lateral photophores distribution) is in favor of sexual and species recognition, while the ventral distribution of photophores, meanwhile, supports the countershading use of light for camouflage purposes (4,20). Myctophid otoliths from the following species—*Electrona antarctica, Electrona carlsbergi* and *Gymnoscopelus nicholsi*—were found in abundance in stomachs of SES from the Kerguelen sector (21) and elsewhere (22). One critical question is how these predators locate their prey in the deep dark ocean, as SESs do not echolocate as cetaceans (23). To date, this question remains unresolved; however, there is some evidence that elephant seals could partly rely on vision to locate their prey in deep waters (15,24). Pinnipeds in general and elephant seals, especially, have some evolved visual abilities (25,26). They have large eyes composed by a retina with a deep sea rhodopsin exhibiting a maximum sensitivity around 470–490 nm (24).

Based on this information, SES should be able to use bioluminescence emission from Myctophids to forage on them. Previous study showed that the foraging intensity of SESs during their dives was positively related to the number of bioluminescence events detected in dives (15). This result could suggest that (i) bioluminescence may provide indications of the biological richness of the area, and therefore indirect clues of prey occurrence. This bioluminescence might be detected and used by SESs to locate their prey. Alternatively or additionally, bioluminescence might be emitted (ii) as a mechanic reaction to SES movement, just as an indirect consequence of its movement (i.e. in response to pressure wave associated with a moving object in the water (12,27)) or (iii) as a defense mechanism to an approaching predator. In particular, it is assumed that a bright flash at close range is produced to startle and/or divert predators, causing them to hesitate as in a form of predator intimidation (the startle effect) (1).

In this previous study, the bioluminescence events were detected from head-mounted light sensors on SES female looking backward. Indeed, these light sensors were initially deployed to address other questions such as the assessment of phytoplankton concentration by measuring light attenuation (28,29). The backward orientation of the light sensor prevented investigating whether the bioluminescence events were occurring prior or after the animal passage and therefore would act as an attractor of the SES or were the consequence of its passage. In addition, bioluminescence events were detected as discontinuities/anomalies into the light signal recorded by a photodiode integrated into classical irradiance time-depth recorder tags, (TDR tags, Wildlife Computers) deployed on SES (15). However, neither calibration of that photodiode nor validation of the correspondence between light anomalies and real bioluminescence events was performed in the previous study. Finally, the foraging intensity of SES was estimated in this previous study by the diving behavior of the animal, which provides only qualitative proxies of the foraging activity at a dive scale (15) and hence avoided the temporal identification of the foraging in a dive.

In that context, the aim of this study was to complement the previous one and in particular to address the question as to whether bioluminescence can be used by SESs as a guide to locate their prey. To address that question, we first tested under experimental conditions the ability of the photodiode integrated into the TDR tags from Wildlife Computers to detect bioluminescence. Then, we investigated the quantitative and chronological link between forward bioluminescence and prey capture attempts (PCAs hereafter), a continuous and quantitative proxy of the foraging activity along dives, detected from the processing of acceleration signal on head-mounted accelerometers (30–34).

MATERIALS AND METHODS

Experimental design for testing the light sensor

The photodiode integrated into classical irradiance time-depth recorder tags (TDR tags, Wildlife Computers) was a Hamamatsu silicon S2387 equipped with a blue window transmittance filter. It was built to measure changes in light under very low light conditions, the light level being measured as an irradiance at a wavelength of 550 nm with a logarithmic range from 5×10^{-12} W cm^{-2} to 5×10^{-2} W cm^{-2} represented by raw values from 10 to 250. Considering that all TDR tags include the same photodiode, we only used one device (one TDR10-X) in the experimental phase. The tag was programmed to sample the light level every one-second.

Spectral sensitivity. The spectral sensitivity of the photodiode was assessed using a 100 W halogen cold light source (Euromex LE 5210) and a monochromator (Oriel—Analis).

The tag was immersed in a few centimeters of seawater (~10–12°C) in a black container. The light source was used to emit a directed white light to the monochromator, while the monochromator was used to transmit a mechanically selectable wavelength of the white light to the tag. The monochromator inlet and outlet apertures of light were fixed to 5 mm. During that experiment, the photodiode was exposed to increasing wavelengths ranging from 360 nm to 660 nm by a 10 nm step every 20 s.

Detection angle. Tag shape and/or epoxy coverage may impact viewing angle of the photodiode, once integrated into the tag, both on the *x*- (Fig. 1) or on the *y*-axis (Fig. 1).

This experiment was intended in assessing the angle of view of the photodiode once integrated into the tag. To do this, once the tag put in a few centimeters of seawater, the two axes (i.e. *x* and *y* Fig. 1) were tested using 19 incidence angles going from −90° to 90° measured against the z-axis (Fig. 1) with 10° step increments. A 465 nm blue-light-emitting diode (i.e. LED) was chosen with an intensity of 700 million of relative light units (i.e. RLU) for the light emission, which corresponds to $1.2 \cdot 10^{-7}$ W cm^{-2}. For each tested angle, the tag was initially put in

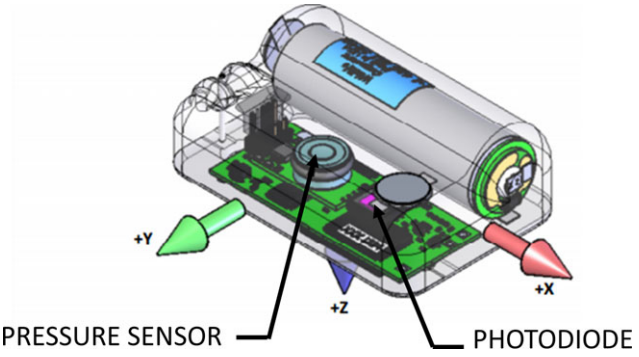

Figure 1. Schema of a TDR10-X with the different axis orientation: x from left to right, y from backward to forward and z from top to bottom. (Wildlife computers: http://wildlifecomputers.com/wp-content/uploads/manuals/MK10-User-Guide.pdf).

the full light condition (ambient light on and LED off) for a few seconds, then in total darkness (ambient light off and LED off), then in the test condition (ambient light off and LED on) and finally in the total darkness condition (ambient light off and LED off).

Detection distance. The distance of detection of the photodiode was estimated using the same LED as previously described (i.e. a 465 nm blue LED with an intensity of $1.2 \cdot 10^{-7}$ W cm^{-2}). The TDR10-X was set up, in a dark room, on the ground against a wall in a container filled with seawater. Seven marks were drawn on the wall at 40 cm, 90 cm, 140 cm, 190 cm, 240 cm, 290 cm and 340 cm to the TDR10-X photodiode to position the LED. Firstly, the photodiode was exposed to the black condition (standard light off and LED off); then, the photodiode was exposed to the test conditions (standard light off and blue LED on) for a distance decreasing from 340 cm to 40 cm with 50 cm increment step. Finally, the photodiode was exposed again to the black condition (standard light off and LED off). Each position of the LED was activated for 5 s, and the photodiode was exposed to the black condition between each new-tested distance.

Measure precision. To estimate the precision of the measurement of light intensity by the photodiode, we exposed it to different constant light condition during several minutes. Regardless of the different constant light condition, the tag was maintained in a dark room and in a container filled with seawater. The first constant light condition was constructed using the previously described blue LED (465 nm and $1.2 \cdot 10^{-7}$ W cm^{-2}) and another blue LED with the same characteristics but with a double neutral filtering (1% and 1‰). The second constant light condition was constructed using only the 1% filtering LED. The third constant light condition was constructed using only the 1‰ filtering LED. Then, the TDR10-X photodiode was exposed to complete darkness. Measure precision was considered in this work as the degree of reproducibility of a measure. For each constant light condition, the measure precision was calculated as the difference between the minimum measure and the maximum one.

Real bioluminescence detection. This experiment aimed to assess whether the light anomalies that we can detect on the light signal recorded by the photodiode when deployed on SES (15) can correspond to natural bioluminescence events. To do so, TDR10-X tag was placed in a seawater container with bioluminescent brittle stars stimulated to emit bioluminescence. One green brittle star (*Ophiopsila californica* λmax 515 nm; J. Mallefet personal communication) and one blue brittle star (*Amphiura arcystata,* λmax 465 nm; J. Mallefet personal communication) were chosen in that experiment because they were easily handled in the laboratory and because their emissions matched the range of expected emission at depth. Over a six minute period, a bright green-emitting brittle star was stimulated twice and then a weak blue-emitting brittle star was stimulated once.

In situ foraging behavior

Ethics statement. Our study on elephant seals was approved and authorized by the ethics committee of the French Polar Institute (Institut Paul Emile Victor—IPEV). This institute does not provide any permit number or approval ID; however, animals were handled and cared for in total accordance with the guidelines and recommendations of this committee (dirpol@ipev.fr).

Deployment of devices. Over three breeding seasons (October/November 2010–2011, 2011–2012 and 2013–2014), 11 postbreeding female SESs were captured at the Kerguelen Islands (49° 20′ S, 70° 20′E) and anesthetized using a 1:1 combination of tiletamine and zolazepam (Zoletil 100) (35). Individuals were then equipped with a range of satellite tags and data loggers.

Animals were equipped with a combination of a Splash-10 tag (Splash-10, Wildlife Computers) and a TDR–accelerometer (TDR10-X, Wildlife Computers). The Splash-10 tags collect and archive dive depth at 1 Hz, while locations are estimated by the orbiting Argos satellites and then transmitted to the user. The TDR10-X is configured with multiple sensors. The first sensor records and archives at 1 Hz, the diving depth. For this, a-bit analog-to-digital converter is used, which provides highly accurate measurements from 0 to +1000 m, with 0.5 m resolutions and an accuracy of ±1% of the reading. In addition, measurements from 1000 to 1500 m are made with a lesser degree of accuracy. The second sensor records and archives at 1 Hz the temperature. For this, a 12-bit analog-to-digital converter is used, providing an actual measured range of −40 to +60°C, with 0.05°C resolution and an accuracy of ±0.1°C. This measure was not used in this study. The third sensor records and archives at 1 Hz light levels using a Hamamatsu silicon photodiode S2387, presented previously. Finally, the last sensor samples and archives at 16 Hz the acceleration of the animal on three axes: longitudinal (surge), vertical (heave) and lateral (roll) axes.

Each TDR10-X tag was firstly glued to the Splash-10 tag. These associations were then glued using quick-setting epoxy (Araldite AW 2101, Ciba) on the head of the 11 seals to measure the light in front of animals with the *x*-axis of the tag oriented from the left to the right of the animal and the *y*-axis of the tag oriented from the top to the bottom of the animal (Fig. 2). Upon returning from their postbreeding foraging trip after 65 to 80 days, females were localized on land via the Argos system and recaptured and the electronic devices were recovered.

Data processing—detection of dives and night/day separation. Dives of the 11 animals were analyzed from the time-depth records (from TDR10-X tags) using a custom-written MATLAB (version 7.0.1) code (available on request). For this, each dive was defined as an excursion over a 15 m depth (33). Then, each detected dive was divided into three distinct phases based on a cubic polynomial function fitted on the time-depth records. The descent and ascent phases were defined when the fitted value of vertical speed (dz/dt) exceeded 0.75 m s^{-1}. The bottom phase was defined as the period between the end of the descent and the beginning of the ascent phases. Finally, each dive was associated with a day or night period. Day period was here considered to encompass the day but also the dawn and the dusk. To do so, we calculated the elevation of the sun (degrees) at the location and the time where the dives occurred (using the package "maptools" (R 2.10.1), function "solarpos"). If the elevation of the sun was lower than −6°, the dive was considered as a night dive and otherwise the dive was considered as a day dive.

Data processing—detection of bioluminescence events. Considering that the ambient light reaches nearly constant low values at depths of 550 m during the day (including dawn and dusk in this study), and 250 m at night (15), any sudden increase in the ambient light level at depths deeper than these limits can be considered as a bioluminescent event around the SES. For this reason, bioluminescence events were only detected from the light signals recorded by the TDR10-X tags at depths deeper than the thresholds aforementioned. To do so, we used a custom-written MATLAB code (version 7.0.1; code available on request). This code used the "findpeaks" function, and we considered a true bioluminescence event only when the threshold height difference between a peak and

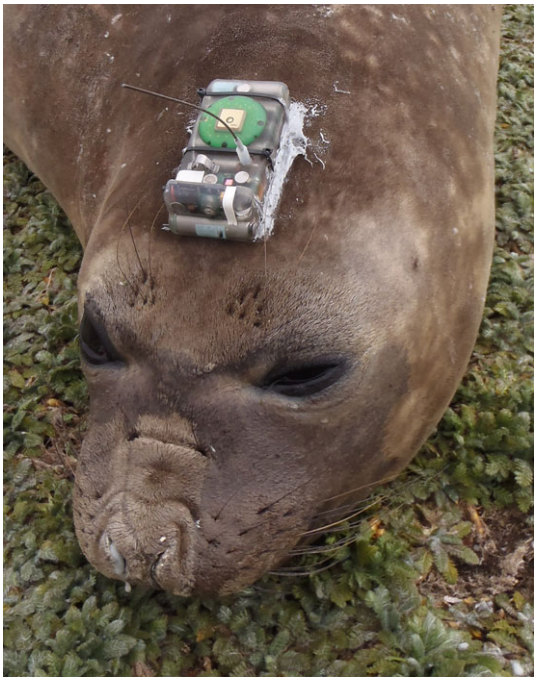

Figure 2. Deployment of a TDR10-X on a female SES. The association of the TDR10-X and the Splash-10 tag was glued on the head of the seal to measure the light in front of animals with the *x*-axis of the tag oriented from the left to the right of the animal and the *y*-axis of the tag oriented from the top to the bottom of the animal.

its previous neighboring values was higher than the precision threshold obtained in the experimental part.

Data processing—detection of prey encounter events. Acceleration data from the 11 individuals were processed according to (32) and (36) (custom-written MATLAB code—available on request). The procedure has been described in detail in (33). Briefly, acceleration records from the TDR10-X tags were first filtered on the three axes to remove "noises" in the signals induced by swimming movement. For each axis, significant peaks in acceleration were then detected when standard deviation of acceleration values within a "5 s" moving window was over a certain threshold. Such a threshold was determined for each axis and each animal using a clustering method where the number of clusters was predefined to 2 (function "kmeans"—tool box statistics—MATLAB). Only peaks above threshold simultaneously detected on the three axes were considered as a PCA.

Statistical analyses. Statistical analyses were carried out at the dive scale. For this reason, the number of PCA and the number of bioluminescence events were counted for each dive. Only dives for which depth exceeded the depth thresholds for the day and night period were kept into analyses. Considering that foraging is mainly related to the bottom phase of a dive (30,37–40), only bioluminescence events and PCA detected at the bottom phase of dives and deeper the depth thresholds aforementioned were included in the analyses. Knowing that the bottom time and the depth of a dive are linked to the foraging activity of animals (15,41), these variables were also taken into account. For this analysis, bottom time was calculated as the time of the bottom exceeding the depth thresholds. For this analysis, we used generalized linear mixed model (nlme package in R 2.10.1, function "glmmPQL"). Due to the fact that the bioluminescence events were detected differently during the day and the night (i.e. depth threshold of 250 m for night dives and 550 for day dives), two models were performed: one for the day and one for the night. Individuals were included as random factors, and we accounted for the temporal correlation in our data using an autoregressive variance–covariance matrix (corAR1). The complete models were built as such: Number of PCA~Bottom time + Depth + Number of bioluminescence event, random = 1|ID, correlation = corAR1 (). The best models for night and day were selected using stepwise likelihood ratio tests.

In parallel to that, statistical analyses were also performed at the bioluminescence event scale. To this end, each bioluminescence event was isolated per dive and the time difference (in seconds) between each of them and the closest PCA was calculated.

RESULTS

Experimental tests of the light sensor

The maximum spectral sensitivity of the photodiode integrated into the TDR10-X tag was found to be 465 nm with a half band width of 50 nm (Fig. 3).

The repeated measures under constant light conditions were found to be constant and equal to 2 in raw values (i.e. $4 \cdot 10^{-13}$ W cm^{-2}). The angular detection ranges of the photodiode were found to be from $-40°$ to $50°$ on the *x*-axis (total angular detection range equal to 90°) and from -50 to $90°$ on the *y*-axis (total angular detection range equal to 140°) (Fig. 4).

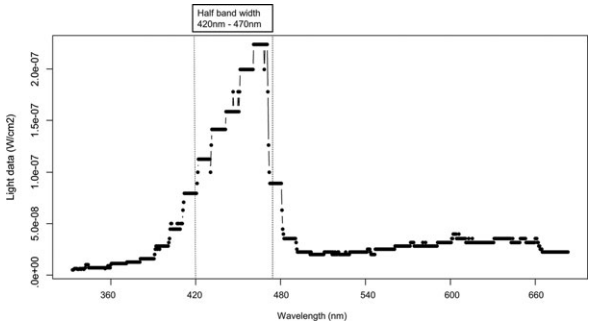

Figure 3. Spectral range of the photodiode included into the TDR10-X. [Color figure can be viewed at wileyonlinelibrary.com]

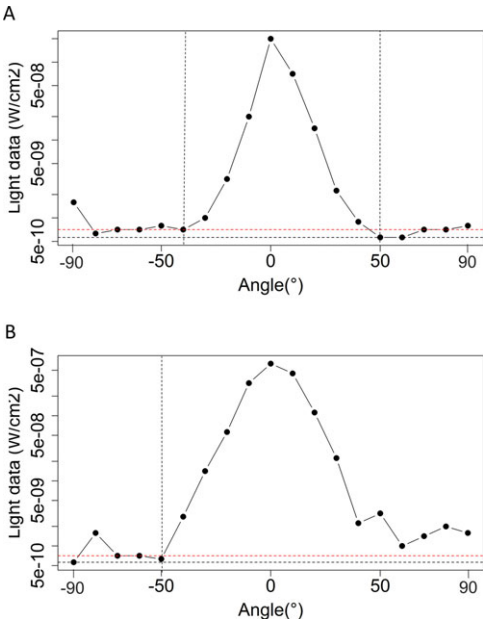

Figure 4. Detection angle of the photodiode included into the TDR10-X. Graphs A and B represent, respectively, the detection angle of the photodiode on the *x*-axis and *y*-axis. The black dotted line corresponds to the darkness condition, and the red dotted line corresponds to the darkness condition to which was added the measure precision.

The maximum detection distance of the photodiode to detect a blue bright light source (i.e. a 465 nm blue LED with an intensity of $1.2 \cdot 10^{-7}$ W cm^{-2}) was found to be 290 cm (Fig. 5).

Finally, the photodiode integrated into the TDR10-X tag was able to detect real bioluminescence events represented by series of flashes and glows from different brittle stars mechanically

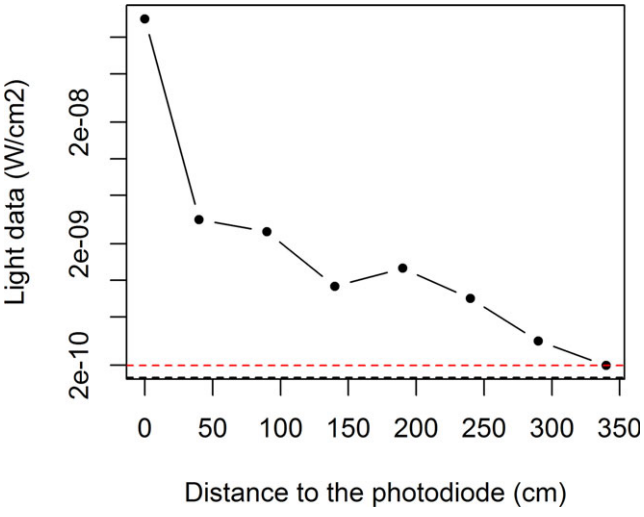

Figure 5. Distance of detection of the photodiode included into the TDR10-X. A 465 nm blue LED with an intensity of 700 million RLU which corresponds to $1.2 \cdot 10^{-7}$ W cm^{-2} was used in that experiment. The black dotted line corresponds to the darkness condition, and the red dotted line corresponds to the darkness condition to which was added the measure precision.

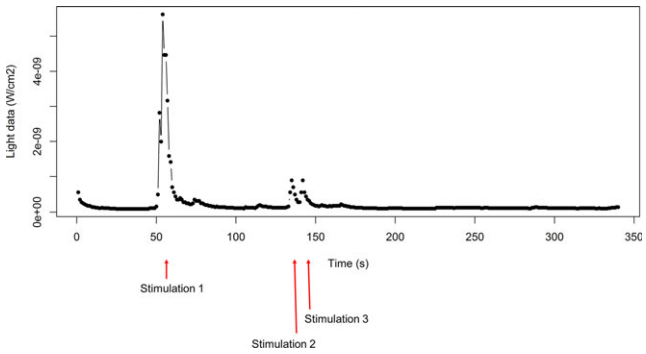

Figure 6. Light profile, measuring by the photodiode included into the TDR10-X and resulting from a three times simulation of brittle stars. [Color figure can be viewed at wileyonlinelibrary.com]

stimulated three times in front of the tag immersed in aquarium (Fig. 6).

In situ foraging behavior

Diving and foraging characteristics of the elephant seals. The 11 female elephant seals spent on average 72.73 ± 8.65 days at sea (Table 1). However, the mean duration TDR10-X records was 32.45 ± 25.68 days (Table 1). A total of 14 218 dives (9249 during the daytime and 4969 during nighttime) were analyzed out of a total of 22 574 dives (see Table 1).

Seventy-five percent of these dives (10 673) were associated with at least one PCA in the bottom phase deeper than the depth thresholds, with a mean of 3.82 ± 4.05 PCAs per bottom phase. A total of 12% of these dives (1680) were associated with at least one bioluminescence event in the bottom phase (i.e. 0.19 ± 0.70 bioluminescence events per bottom phase). However, when at least one bioluminescent event was detected during the bottom phase of the dive, the mean number of bioluminescent events was 1.59 ± 1.54 and 1.60 ± 1.16 for day and for nighttime periods, respectively.

Statistical analyses. At the dive scale. The number of PCA, in a dive, was positively related to the number of bioluminescence events in that dive, and this, both for daytime and nighttime periods (Table 2 and Fig. 7). The results are summarized in the Table 2.

At the bioluminescence event scale. Considering the maximum distance detection of the photodiode, estimated at 290 cm in the experimental part and the mean speed of an SES estimated to be approximately 1 m/s, only the differences under 3 s were conserved. This represents 37% of the detected bioluminescence events, which is much higher than expected just by chance ($W = 121$, $P < 0.001$). Among these events, 69% occurred simultaneously to a PCA, 19% of them took place prior to a PCA and 12% of them took place after a PCA.

DISCUSSION

A light sensor adapted to the study of the bioluminescence

In this study, we experimentally showed that the photodiode integrated into the TDR10-X has the ability to detect events of light emitted by bioluminescent organisms. This result strongly supports the idea that this sensor is able to record *in situ* bioluminescence. We showed then that the sensor sensitivity ranges from 400 to 490 nm, with a maximal sensitivity to 465 nm and a half band width between 420 and 470 nm. Numerous pelagic taxa such as dinoflagellates, jellyfishes, krill, crustaceans, squids and fishes emit bioluminescence mostly within this wavelength window (1,2). Consequently, equipping SES with such a light sensor could provide important information on the horizontal and vertical distribution of bioluminescence within the Southern Ocean. Among all of these bioluminescent organisms, we are particularly interested in Myctophids, known to represent one of the major prey items of SES from Kerguelen Islands (16), with the most common myctophids species in their diet being *Gymnoscopelus nicholsi, Electrona antarctica and Electrona calsbergi* (21,22). Assuming from literature that myctophids emit light with maximal wavelengths ranging from 450 to 480 nm (17–19), the photodiode we used has the ability to detect bioluminescence emissions from these Myctophids species.

Despite the fact that the photodiode allows the *in situ* observation of a large range of bioluminescence events, this sensor is not specific enough to be able to distinguish between different sources (i.e. organisms) of bioluminescence. Moreover, the low sampling frequency of the sensor (respectively, 1 Hz) and limited detection range (<3 m) are likely to induce an undersampling of bioluminescence events such as very short (fast flashes) and low-energy ones,

Table 1. Descriptive statistics of the elephant seal tracks.

Individual ID	Date of deployment	Duration (days)	Duration of TDR10-X (days)	Number of dives	Number of analyzed dives	Number of analyzed dives with at least one PCA	Number of dives with at least one bioluminescence event	Total number of detected PCA	Total number of bioluminescence events
2010–18	26.10.2010	60	60	3361	2479	2053	510	8841	717
2010–19	31.10.2010	80	80	4123	2258	1018	227	4144	240
2010–21	18.11.2010	73	73	4515	2170	1776	401	10487	466
2011–16	26.10.2011	87	10	653	426	367	34	1900	75
2011–18	26.10.2011	66	12	1030	534	439	24	2423	47
2011–27	30.10.2011	79	14	1229	753	500	73	1684	150
2013–1	28.10.2013	75	25	1724	1359	1185	87	7096	195
2013–3	29.10.2013	81	23	1583	1175	1038	78	7207	164
2013–4	29.10.2013	64	18	1256	798	485	62	2285	238
2013–6	29.10.2013	72	16	1284	863	663	106	3666	221
2013–7	30.10.2013	63	26	1816	1403	1149	78	4590	140

Table 2. Results of models of the variation of PCA according to bottom time, maximum depth and the number of bioluminescence events both for night- and daytime periods.

	Night dives		Day, dawn and dusk dives	
Parameters	Coefficient	*P*-value	Coefficient	*P*-value
Intercept	1.33E+00	<0.001	8.70E-01	<0.001
Bottom Time	−1.17E-01	<0.001	3.40E-01	<0.001
Maximum depth	−2.50E-01	2.90E-02	-1.10E-01	<0.001
Number of bioluminescence events	4.80E-02	<0.001	3.00E-02	<0.001

which could be the most common ones. Consequently, our results should be considered at least as an underestimation of all bioluminescent events encountered by SES.

This leads us to discuss the nature of the current detected events. It is important to note that bioluminescence can be of two sorts. While fast flashes (<2 s) are used generally for communication (i.e. intraspecific and sex identification) or to startle potential predators, glow emissions (>2 s) are classically used to attract prey or to mask the fish silhouette from predators underneath (counter illumination) (1,42,43). Despite the fact that these two types of bioluminescence events are not characterized by specific intensities, it is often observed, and principally due to their functions, that the fast flashes are bright, while the glows are characterized by a low intensity (1,42,43). Because of the capabilities of the photodiode and especially the frequency of the measurement, we believe that the vast majority of the glows met by SES with a wavelength into the sensor detection range are detected by the photodiode, while the flashes are likely to be significantly undersampled because of their low duration (<2 s). Therefore, future research should use a higher sampling rate with more sensitive photodiodes or photomultipliers as performed in (44).

Bioluminescence cause or reaction of the SES foraging activity?

Our results showed a positive relationship between bioluminescence and foraging activity of SES both during day and night. These new results confirm those previously obtained on the qualitative relationship between the foraging intensity, estimated from the diving behavior of SES, and the bioluminescence (15). But these new results highlight also a quantitative relationship between bioluminescence and PCA. Our initial hypothesis was based on the idea that the detected bioluminescence events were those of Myctophids hunted by SES. However, SESs from Kerguelen area are known to forage also on other types of prey such as cephalopods (21,45) including some bioluminescent species. Thus, considering the large number of bioluminescence sources which can be detected by the light sensor, we cannot exclude that bioluminescent events recorded by the sensor and linked to PCA might be emitted by other SES prey such as cephalopods or even from organisms not hunted by SES but living in the same ecological niche as SES prey.

This quantitative relationship between bioluminescence and PCA leads to a new stage to understand more precisely the interspecies interactions using bioluminescence. However, it is important to note that nothing leads us to rule whether (i) SES intentionally moves to feed toward areas exhibiting high levels of bioluminescence or (ii) bioluminescent organisms emit bioluminescence as a mechanic reaction to the SES motion activity or (iii) bioluminescent organisms emit bioluminescence as a defense mechanism to an approaching predator. The fact that bioluminescence was detected frontward is in line with the possibility that bioluminescence would preexist in the area before its passage. However, the limited capacities of the photodiode and principally its restricted detection distance of 290 cm do not allow us to address correctly this issue. Without information from the bioluminescent area beyond three meters, we are not able to distinguish between these three assumptions. To answer this question, further

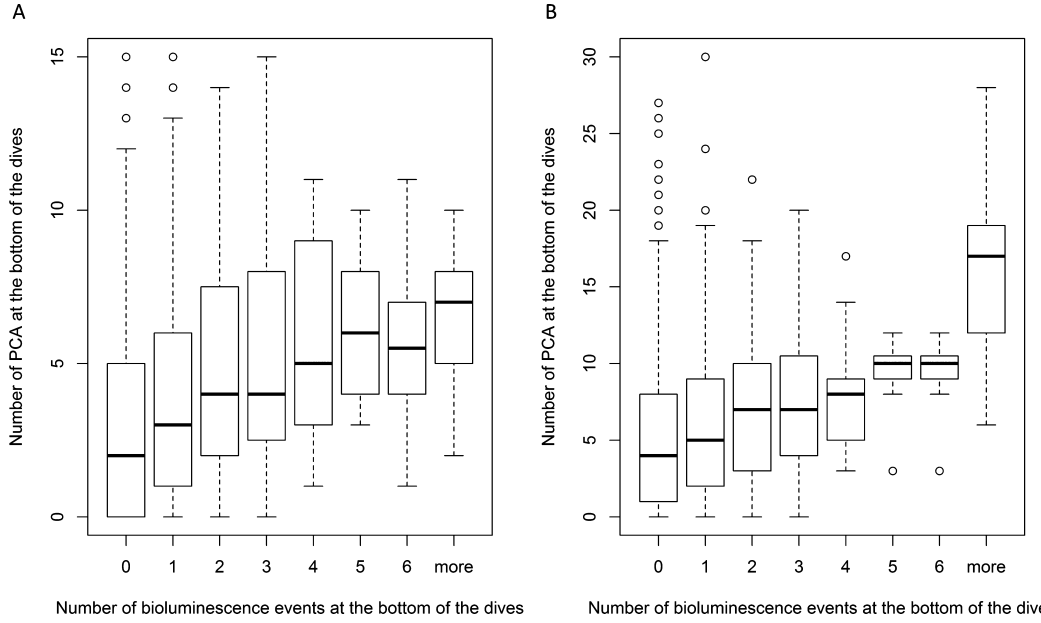

Figure 7. Number of bioluminescence events detected in the bottom of a dive in function of the number of PCA per bottom. Graph A represents this relationship in day period, and the graph B represents this relationship during the night.

research is needed using new loggers allowing the three-dimensional reconstruction of the SES trajectory during dives in combination with new highly sensitive light sensors (allowing an improved distance detection and higher sampling rate) and accelerometers. Furthermore, highly sensitive cameras triggered by bioluminescence flashes could characterize the type of bioluminescent organisms. The objectives of this further work might be studying the succession of the three following phenomena: changes in direction, bioluminescence events and PCA. Such work would move forward in the understanding of a possible use of bioluminescence in the foraging behavior of the predator.

Despite the fact that the limited detection distance and sampling rate of the photodiode prevent us to obtain a full description of bioluminescent events, the new results bring new insights. Indeed, a total of 37% of the bioluminescence events occurred within 3-s of a PCA, which is much higher than expected just by chance and which suggests a functional link between bioluminescence and predation of SES. Furthermore, the vast majority of them (69%) were detected exactly at the same time as a PCA, which is in line with the fact that bioluminescence could be a mechanic reaction of the predator activity. Nevertheless, 19% of them preceded a PCA, which signifies that bioluminescence was present before the beginning of the foraging activity and hence could be used as an attractive event for the SES. However, it is noteworthy that PCA occurred also during dive in the absence of detected bioluminescence events (Fig. 7). As already mentioned, the photodiode could miss some bioluminescence events in the case where they were outside the detection range or the viewing angles of the sensor or even if they were too short in duration. It is also possible that not all SES prey is bioluminescent, as we mentioned previously, and would explain why PCA could be detected without bioluminescence. At this stage, to determine whether bioluminescence is used by SES to detect their prey or is emitted as mechanism response or as a defense behavior in response to the SES passage remains a challenge, and it is rather likely that both three assumptions are true.

Bioluminescence is a common feature of the marine environment. It constitutes the only source of light at deep depth and for moonless nights. Therefore, deep diving mammals are likely to key on bioluminescence organisms when searching for prey. Despite the fact that our study was focused on a possible role of the vision in foraging activity of SES, it is possible that SESs rely on other sensory channels to locate their prey. Pinnipeds, which do not echolocate, have to rely on other senses to detect and locate their prey. For instance, they are known to rely on the tactile sense of their innervated facial vibrissae or whiskers for underwater orientation and foraging by detecting vibration fields produced by moving prey (46). Audition is another likely candidate to locate prey fields. Indeed, elephant seals have very good hearing abilities and detect sounds better under water than in air (47). With all these possibilities, it is likely that SESs rely on hierarchical and multisensorial channels such as hearing, vision and tactile senses to detect and locate their preys. Hearing is likely to be used at larger scale than vision and the vibrissae vibrations detection, which may only be efficient at short ranges.

CONCLUSION

In this study, we chronologically investigated the detected bioluminescence events with the foraging ones. We showed that the bioluminescence was positively related to PCA, which comforted the previous results. Theoretically, it could have been possible to determine whether the detection of bioluminescence takes place before or after the foraging. However, the measurement range of the photodiode is being limited to less than 3 m around the moving animal, and this did not allow to investigate whether the bioluminescence was present long before the foraging. Nevertheless, we managed to determine the chronology of the events within a period of 3 s. These results remain promising but they highlight the need to develop more powerful and sensitive bioluminescence devices in order to be able to accurately report on the relationships existing between bioluminescence and organisms *in situ*.

Acknowledgements—The authors would like to thank the IPEV logistical staff as well as all the colleagues and volunteers for their work in the field, with the special acknowledgment of the invaluable field contribution of N. El Ksabi and G. Bessigneul.

REFERENCES

1. Haddock, S. H. D., M. A. Moline and J. F. Case (2010) Bioluminescence in the sea. *Annu. Rev. Mar. Sci.* **2**, 443–493.
2. Turner, J. R., E. M. White, M. A. Collins, J. C. Partridge and R. H. Douglas (2009) Vision in lanternfish (Myctophidae): adaptations for viewing bioluminescence in the deep-sea. *Deep-Sea Res. I* **56**, 1003–1017.
3. Widder, E. A. (2010) Bioluminescence in the ocean: origins of biological, chemical, and ecological diversity. *Science* **328**, 704–708.
4. Herring, P. J. (2007) Sex with the lights on? A review of bioluminescent sexual dimorphism in the sea. *J. Mar. Biol. Assoc. U.K.* **87**, 829–842.
5. Widder, E. A. (1999) Bioluminescence. In *Adaptive Mechanisms in the Ecology of Vision* (Edited by S. N. Archer, M. B. A. Djamgoz, E. Loew, J. C. Partridge and S. Vallerga), pp. 555–581. Kluwer Academic, Dordrecht, the Netherlands.
6. Johnsen, S., E. A. Widder and C. D. Mobley (2004) Propagation and perception of bioluminescence: factors affecting counterillumination as a cryptic strategy. *Biol. Bull.* **207**, 1–16.
7. Claes, J. M. and J. Mallefet (2008) Early development of bioluminescence suggests camouflage by counter-illumination in the velvet belly lantern shark *Etmopterus spinax* (Squaloidea: Etmopteridae). *J. Fish Biol.* **73**, 1337–1350.
8. Claes, J. M. and J. Mallefet (2010) The lantern shark's light switch: turning shallow water crypsis into midwater camouflage. *Biol. Lett.* **6**, 685–687.
9. Mesinger, A. F. and J. F. Case (1992) Dinoflagellate luminescence increases susceptibility of zooplankton to teleost predation. *Mar. Biol.* **112**, 207–210.
10. Hanley, K. A. and E. A. Widder (2017) Bioluminescence in Dinoflagellates: evidence that the adaptive value of bioluminescence in Dinoflagellates is concentration dependent. *Photochem. Photobiol.* **93**, 519–530.
11. Widder, E., S. Bernstein, D. Bracher, J. Case, K. Reisenbichler, J. Torres and B. Robison (1989) Bioluminescence in the Monterey submarine canyon: image analysis of video recordings from a midwater submersible. *Mar. Biol.* **100**, 541–551.
12. Craig, J., A. J. Jamieson, A. Heger and I. G. Priede (2009) Distribution of bioluminescent organisms in the Mediterranean Sea and predicted effects on a deep-sea neutrino telescope. *Nucl. Instrum. Meth. Phys. Res. A* **602**, 224–226.
13. Craig, J., I. G. Priede, J. Aguzzi, J. B. Company and A. J. Jamieson (2015) Abundant bioluminescent sources of low-light intensity in the deep Mediterranean Sea and North Atlantic Ocean. *Mar. Biol.* **162**, 1637–1649.
14. Campagna, C., J. Dignani, S. B. Blackwell and M. R. Marin (2001) Detecting bioluminescence with an irradiance time depth recorder deployed on southern elephant seals. *Mar. Mammal Sci.* **17**, 402–414.
15. Vacquié-Garcia, J., F. Royer, A. C. Dragon, M. Viviant, F. Bailleul and C. Guinet (2012) Foraging in the darkness of the Southern

Ocean: influence of Bioluminescence on a deep diving predator. *PLoS ONE* **7**(8), e43565.
16. Cherel, Y., S. Ducatez, C. Fontaine, P. Richard and C. Guinet (2008) Stable isotopes reveal the trophic position and mesopelagic fish diet of female southern elephant seals breeding on the Kerguelen Islands. *Mar. Ecol. Prog. Ser.* **370**, 239–247.
17. Widder, E. A., M. I. Latz and J. F. Case (1983) Marine Bioluminescence spectra measured with an optical multichannel detection system. *Biol. Bull.* **165**(3), 791–810.
18. Herring, P. J. (1983) The spectral characteristics of luminous marine organisms. *P. Roy. Soc. B-Biol. Sci.* **220**, 183–217.
19. Mallefet, J., J. Vacquié-Garcia, F. Bailleul and C. Guinet (2014) Are southern elephant seals attracted by the bioluminescence of lantern fishes in the deep dark of the southern Ocean? Abstract 14th Benelux Congress of Zoology, Liège, p. 201.
20. Davis, M. P., N. I. Holcroft, E. O. Wiley, J. S. Sparks and W. Leo Smith (2014) Species-specific bioluminescence facilitates speciation in the deep sea. *Mar. Biol.* **161**, 1139–1148.
21. Slip, D. J. (1995) The diet of southern elephant seals (*Mirounga leonina*) from Heard Island. *Can. J. Zool.* **73**, 1519–1528.
22. Daneri, G. A. and A. R. Carlini (2002) Fish prey of southern elephant seals, *Mirounga leonina*, at King George Island. *Polar Biol.* **25**, 739–743.
23. Schusterman, R. J., D. Kastak, D. H. Levenson, C. J. Reichmuth and B. L. Sout-hall (2000) Why pinnipeds don't echolocate. *J. Acoust. Soc. Am.* **107**, 2256–2264.
24. Lythgoe, J. N. and H. J. A. Dartnall (1970) A deep Sea ''Rhodopsin'' in a Mammal. *Nature* **227**, 955–956.
25. Levenson, D. H. and R. J. Schusterman (1997) Pupillometry in seals and sea lions: Ecological implication. *Can. J. Zool.* **75**, 2050–2057.
26. Levenson, D. H. and R. J. Schusterman (1999) Dark adaptation and visual sensitivity in shallow and deep diving pinnipeds. *Mar. Mam. Sci.* **15**, 1303–1313.
27. Herring, P. J. (1998) Bioluminescence: dolphins glow with the flow. *Nature* **393**, 731–733.
28. Jaud, T., A. C. Dragon, J. Vacquie-Garcia and C. Guinet (2012) Relationship between chlorophyll a concentration, light attenuation and diving depth of the southern elephant seal *Mirounga leonina*. *PLoS ONE* **7**(10), e47444.
29. Bayle, S., P. Monestiez, C. Guinet and D. Nerini (2015) Moving toward finer scales in oceanography: predictive linear functional model of Chlorophyll a profile from light data. *Prog. Oceanogr.* **134**, 221–231.
30. Wilson, R. P., A. Steinfurth, Y. Ropert-Coudert, A. Kato and M. Kurita (2002) Lipreading in remote subjects: an attempt to quantify and separate ingestion, breathing and vocalisation in free-living animals using penguins as a model. *Mar. Biol.* **140**, 17–27.
31. Suzuki, I., Y. Naito, L. P. Folkow, N. Miyazaki and A. S. Blix (2010) Validation of a device for accurate timing of feeding events in marine animals. *Polar Biol.* **32**, 667–671.
32. Viviant, M., A. W. Trites, D. A. S. Rosen, P. Monestiez and C. Guinet (2010) Prey capture attempts can be detected in Steller sea lions and other marine predators using accelerometers. *Polar Biol.* **33**, 713–719.
33. Guinet, C., J. Vacquié-Garcia, B. Picard, G. Bessigneul, Y. Lebras, A. C. Dragon, M. Viviant, J. P. Y. Arnould and F. Bailleul (2014) Southern Elephant Seal foraging success in relation to temperature and light conditions: insight on their prey distribution. *Mar. Ecol. Prog. Ser.* **499**, 285–301.
34. Richard, G., S. L. Cox, B. Picard, J. Vacquie-Garcia and C. Guinet (2016) Southern elephant seals replenish their lipid reserves at different rates according to foraging habitat. *PLoS ONE* **11**(11), e0166747.
35. McMahon, C. R., H. R. Burton, S. McLean, D. J. Slip and M. N. Bester (2000) Field immobilisation of southern elephant seals with intravenous tiletamine and zolazepam. *Vet. Rec.* **146**, 251–254.
36. Gallon, S., F. Bailleul, J. B. Charrassin, C. Guinet, C. A. Bost, Y. Handrich and M. Hindell (2012) Identifying foraging events in deep diving southern elephant seals, *Mirounga leonina*, using acceleration data loggers. *Deep-Sea Res.* **88–89**, 14–22.
37. Watanabe, Y., Y. Mitani, K. Sato, M. F. Cameron and Y. Naito (2003) Dive depths of Weddell seals in relation to vertical prey distribution as estimated by image data. *Mar. Ecol. Prog. Ser.* **252**, 283–288.
38. Austin, D., W. D. Bowen, J. I. McMillan and D. J. Boness (2006) Stomach temperature telemetry reveals temporal patterns of foraging success in a free-ranging marine mammal. *J. Anim. Ecol.* **75**, 408–420.
39. Fossette, S., P. Gaspar, Y. Handrich, Y. Le Maho and J. Y. Georges (2008) Dive and beak movement patterns in leatherback turtles *Dermochelys coriacea* during internesting intervals in French Guiana. *J. Anim. Ecol.* **77**, 236–246.
40. Kuhn, C. E., D. E. Crocker, Y. Tremblay and D. P. Costa (2009) Time to eat: measurements of feeding behaviour in a large marine predator, the northern elephant seal *Mirounga angustirostris*. *J. Anim. Ecol.* **78**, 513–523.
41. Dragon, A. C., A. Bar-Hen, P. Monestiez and C. Guinet (2012) Horizontal area-restricted-search and vertical diving movements to predict foraging success in a marine top-predator. *Mar. Ecol. Prog. Ser.* **447**, 243–257.
42. Young, R. E. and F. M. Mencher (1980) Bioluminescence in mesopelagic squids: Diel color change during counterillumination. *Science* **208**, 1286–1288.
43. Herring, P. J., E. A. Widder and S. H. D. Haddock (1992) Correlation of bioluminescence emissions with ventral photophores in the mesopelagic squid Abralia veranyi (Cephalopoda: Enoploteuthidae). *Mar. Biol.* **112**, 293–298.
44. Cronin, H. A., J. H. Cohen, J. Berge, G. Johnsen and M. A. Moline (2016) Bioluminescence as an ecological factor during high Arctic polar night. *Sci. Rep.* **6**, 36374. https://doi.org/10.1038/srep36374.
45. Rodhouse, P. G., T. R. Arnbom, M. A. Fedak, J. Yeatman and A. W. A. Murray (1992) Cephalopod prey of the southern elephant seal, *Mirounga leonina* L. *Can. J. Zool.* **70**, 1007–1015.
46. Dehnhardt, G., B. Mauck, W. Hanke and H. Bleckmann (2001) Hydrodynamic trail following in harbor seals (*Phoca vitulina*). *Science* **293**, 102–104.
47. Kastak, D. and R. J. Schusterman (1998) In-air and underwater hearing sensitivity of a northern elephant seal (*Mirounga angustirostris*). *Can. J. Zool.* **77**, 1751–1758.